MOLECULAR AND CELLULAR BIOLOGY, Apr. 2004, p. 2779–2788 Vol. 24, No. 7
0270-7306/04/$08.00+0 DOI: 10.1128/MCB.24.7.2779–2788.2004

Mdt1, a Novel Rad53 FHA1 Domain-Interacting Protein, Modulates DNA Damage Tolerance and G_2/M Cell Cycle Progression in *Saccharomyces cerevisiae*

Brietta L. Pike,[1,2] Suganya Yongkiettrakul,[3] Ming-Daw Tsai,[3] and Jörg Heierhorst[1,2]*

St. Vincent's Institute of Medical Research[1] and Department of Medicine, St. Vincent's Hospital,[2] The University of Melbourne, Fitzroy, Victoria 3065, Australia, and Departments of Chemistry and Biochemistry, The Ohio State University, Columbus, Ohio 43210[3]

Received 18 November 2003/Returned for modification 22 December 2003/Accepted 5 January 2004

The Rad53 kinase plays a central role in yeast DNA damage checkpoints. Rad53 contains two FHA phosphothreonine-binding domains that are required for Rad53 activation and possibly downstream signaling. Here we show that the N-terminal Rad53 FHA1 domain interacts with the RNA recognition motif, coiled-coil, and SQ/TQ cluster domain-containing protein Mdt1 (YBl051C). The interaction of Rad53 and Mdt1 depends on the structural integrity of the FHA1 phosphothreonine-binding site as well as threonine-305 of Mdt1. Mdt1 is constitutively threonine phosphorylated and hyperphosphorylated in response to DNA damage in vivo. DNA damage-dependent Mdt1 hyperphosphorylation depends on the Mec1 and Tel1 checkpoint kinases, and Mec1 can directly phosphorylate a recombinant Mdt1 SQ/TQ domain fragment. *MDT1* overexpression is synthetically lethal with a *rad53* deletion, whereas *mdt1* deletion partially suppresses the DNA damage hypersensitivity of checkpoint-compromised strains and generally improves DNA damage tolerance. In the absence of DNA damage, *mdt1* deletion leads to delayed anaphase completion, with an elongated cell morphology reminiscent of that of G_2/M cell cycle mutants. *mdt1*-dependent and DNA damage-dependent cell cycle delays are not additive, suggesting that they act in the same pathway. The data indicate that Mdt1 is involved in normal G_2/M cell cycle progression and is a novel target of checkpoint-dependent cell cycle arrest pathways.

The integrity of eukaryotic genomes is monitored by remarkably conserved checkpoint signaling pathways that arrest the cell cycle in the presence of DNA damage, replication blocks, and mitotic spindle defects and activate repair processes in order to ensure precise DNA replication, chromosome segregation, and subsequent formation of viable progenitor cells. Defects in checkpoint mechanisms can lead to genomic instability and predispose multicellular organisms to cancer (53). Human genetic disorders that have an increased propensity for cancer and that are linked to mutations in checkpoint genes include ataxia telangiectasia (AT), caused by mutations in the AT-mutated (ATM) kinase (1); Nijmegen breakage syndrome, caused by mutations in the BRCT and FHA domain-containing Nbs1 protein (6); and Li-Fraumeni multicancer syndrome, caused by mutations in the tumor suppressor p53 or Chk2 kinase (4).

Studies with *Saccharomyces cerevisiae* have been instrumental to the understanding of molecular mechanisms of checkpoint pathways. For example, the tumor suppressor Chk2 kinase was only rather recently identified in searches for human orthologs of Rad53 (32), which plays a central role in *S. cerevisiae* checkpoint responses (reviewed in reference 53). Rad53 activation through phosphorylation depends on three major pathways that act in concert with the Mec1/Lcd1 complex (orthologs of human ATM/ATR and ATRIP) (7, 8, 40). Two partially overlapping Rad53 activation pathways, one consisting of Rad17, Rad24, Mec3, and Ddc1 (24) and the other containing the Rad9 protein (9), operate throughout the cell cycle, whereas a third pathway, involving Pol2, Dpb11, Drc1, Rfc5, and Mrc1, specifically monitors the progress of DNA replication and damage during S phase (2, 34). Damage-induced Rad53 activation leads to G_1/S delay through inhibition of the Swi6 transcription factor involved in *CLN1/2* cyclin expression (45), inhibition of Dbf4/Cdc7 kinase-dependent late replication origin "firing" to delay S-phase progression (41), and G_2/M arrest through inhibition of the Polo-like kinase Cdc5 and the anaphase-promoting complex (39). In addition, Rad53 is involved in the transcriptional induction of DNA repair genes, such as ribonucleotide reductase (RNR) subunits (21); the direct regulation of repair proteins, such as Rad55 (3); chromatin assembly (15); and redistribution of the Ku70/80 and Sir2/3 silencing factors to sites of DNA damage (31). Rad53 is also essential for growth in unperturbed cell cycles through the regulation of deoxynucleoside triphosphate levels during S phase, but *rad53*Δ lethality can be suppressed by overexpression of RNR subunits or deletion of the RNR inhibitor and Rad53 target Sml1 (52). Conversely, as Rad53 is crucial for checkpoint-induced cell cycle arrest, downregulation of its activity is a target for antagonistic pathways that facilitate cell cycle reentry in the adaptation to limited DNA damage (35) or the recovery from arrest after successful DNA damage repair (27).

Rad53 belongs to the conserved family of FHA domain-containing checkpoint kinases, including mammalian Chk2, *S. cerevisiae* Dun1 and Mek1, and *Schizosaccharomyces pombe* Cds1. FHA domains are modular protein-protein interaction domains that preferentially bind to phosphothreonine (pThr) residues in target peptides (reviewed in references 12, 18, and

* Corresponding author. Mailing address: SVIMR, 9 Princes St., Fitzroy, Victoria 3065, Australia. Phone: 61-3-9288-2503. Fax: 61-3-9416-2676. E-mail: heier@ariel.its.unimelb.edu.au.

TABLE 1. Yeast strains used in this study[a]

Strain	Genotype	Reference or source
Y53	*MAT***a** *ade2-1 can1-100 leu2-3,112 trp1-1 ura3-1 sml1*::*HIS3*	52
Y54	Y53 *rad53*::*HIS3 sml1-1*	52
Y57	Y53 *rad53-R70A*	36
Y59	Y53 *rad53-K227A*	36
Y60	Y53 *rad53*::*URA3*	36
Y109	Y53 *mdt1*::*LEU2*	This study
Y110	Y53 *rad53-R70A mdt1*::*LEU2*	This study
Y112	Y53 *rad53*::*URA3 mdt1*::*LEU2*	This study
Y117	Y53 *rad53-K227A mdt1*::*LEU2*	This study
Y122	Y53 *rad9*::*LEU2*	This study
Y123	Y53 *rad53-R70A rad9*::*LEU2*	This study
Y125	Y53 *rad17*::*TRP1*	This study
Y160	Y53 *rad17*::*TRP1 mdt1*::*LEU2*	This study
Y185	Y53 *rad9*::*URA3 mdt1*::*LEU2*	This study
Y186	Y53 *rad9*::*URA3 mdt1*::*LEU2 rad53-R70A*	This study
Y187	Y53 *lcd1*::*LEU2*	38
Y188	Y53 *lcd1*::*LEU2 mdt1*::*TRP1*	This study
Y189	Y53 *MDT1-myc*	This study
Y198	Y53 *mdt1-T305A*	This study
Y208	Y53 *MDT1-myc mec1*::*klURA3*	This study
Y218	Y53 *mdt1-T305A rad17*::*TRP1*	This study
Y272	Y53 *MDT1-myc chk1*::*klURA3*	This study
Y274	Y53 *MDT1-myc rad53*::*klURA3*	This study
Y343	Y53 *MDT1-myc mec1*::*klURA3 tel1*::*KAN*	This study

[a] Y53 is the wild type. *kl*, *Kluyveromyces lactis*.

28). Rad53 contains two FHA domains, flanking the protein kinase catalytic domain. Both FHA domains are required for DNA damage-dependent Rad53 activation and possibly subsequent downstream signaling in vivo (37, 43). Interaction of the C-terminal FHA domain (FHA2) with phosphorylated Rad9 is critical for Rad53 activation (42, 46). A number of proteins—Rad9 (13), Dbf4 (11), Asf1 (43), and Ptc2/3 (27)—have been proposed as candidate ligands for the N-terminal Rad53 FHA1 domain, but it is likely that additional FHA domain-interacting proteins are involved in the wide range of Rad53 functions.

Here we describe a novel pThr-containing protein that specifically interacts with the pThr-binding site of the Rad53 FHA1 domain. Based on DNA damage response phenotypes associated with its deletion, we have termed this protein Mdt1 (for modifier of damage tolerance). Mdt1 is hyperphosphorylated in a checkpoint-dependent manner after DNA damage, and the *MDT1* gene exhibits a number of genetic interactions with checkpoint components. Mdt1 is required for normal G_2/M cell cycle progression in the absence of DNA damage. Altogether, our data indicate that Mdt1 is a novel target of cell cycle arrest checkpoints.

MATERIALS AND METHODS

Yeast strains and plasmids. All yeast strains used in functional experiments (Table 1) were derived from W303-1A strain U952-3B (that is *RAD5*) containing the *sml1*Δ mutation (52), except for a W303-1A *MEC1-myc* strain that was *SML1* (38). *rad53* alleles with FHA1 and kinase catalytic domain mutations were described before (36, 37), and *MDT1-myc* and *mdt1-T305A* alleles were generated by using similar PCR-based site-directed mutagenesis procedures. Gene disruptions were constructed by using standard PCR-based strategies (5) and confirmed by colony PCR. The *MDT1-myc mec1*Δ *tel1*Δ strain was obtained by sporulation and tetrad dissection of a heterozygous diploid W3030 strain (*MAT***a**/*MAT*α *MDT1-myc*/*mdt1*::*LEU2 MEC1*/*mec1*::*klURA3 TEL1*/*tel1*::*KAN SML1*/*sml1*::*HIS3*). Yeast two-hybrid analyses were performed with PJ69-4A (*MAT***a** *trp1-901 leu2-3,112 ura3-52 his3-200 gal4*Δ *gal80*Δ *LYS2*::*GAL1-HIS3 GAL2-ADE2 met2*::*GAL7-lacZ*) (22). For overexpression under the control of the *GAL1* promoter, the *MDT1* open reading frame was fused by PCR to a C-terminal myc tag and cloned into p416-*GAL1*. For expression under the control of its own promoter from a centromeric plasmid, PCR products containing positions −500 to −1 of *MDT1* and the full-length open reading frame fused to a C-terminal myc tag were cloned into the SacI and SmaI sites of pRS416. Correct sequences were confirmed by cDNA sequence analysis. Yeast transformations were performed by using lithium acetate-polyethylene glycol 3350. Untransformed strains were grown in YPD (1% yeast extract, 2% peptone, 2% glucose); plasmid-transformed strains were grown in synthetic complete medium lacking uracil. For repression of the *GAL1* promoter, the medium contained 2% sucrose; for induction, the medium contained 2% sucrose plus 4% galactose. All incubations were performed at 30°C.

HU, MMS, and UV sensitivity assays. For drop tests, 2 μl of 10-fold serial dilutions (starting A_{600}, 0.5) of yeast cultures were spotted onto plates containing hydroxyurea (HU) or methylmethane sulfonate (MMS) or spotted onto YPD, UV irradiated by using a Uvitec CL-508 cross-linker (λ, 254 nm) with a single light bulb at various doses, and incubated for 3 days. For liquid assays, overnight cultures were diluted to an A_{600} of 0.15 and grown for 3 h before the addition of MMS or HU. Aliquots were removed immediately before and at 3 h after the addition of MMS or at 2-h intervals over a 12-h period after the addition of 100 mM HU and plated on YPD. Colonies were counted after 3 days, and survival rates were determined as colonies formed in damage-treated samples as a percentage of colonies formed in relevant untreated samples in ≥3 independent experiments.

Yeast two-hybrid analyses. PJ69-4A cells were cotransformed with plasmid pAS2 (36), encoding a Gal4 DNA-binding domain (BD)– Rad53 FHA1 domain fusion protein (residues 20 to 164), and an *S. cerevisiae* cDNA library fused to the Gal4 activation domain (AD) in pGADGH (17). Transformation mixtures were plated on synthetic complete medium lacking Leu and Trp to select for the two plasmids as well as His and Ade to select for interacting clones that restored Gal4 activity and activated the transcription of the *GAL1-HIS3* and *GAL2-ADE2* reporter genes. All reporter plates also contained 10 mM 3-amino-1,2,4-triazole to provide tighter control of the *HIS3* reporter. A positive interaction was confirmed by retransformation assays of plasmid pGADGH-*MDT1*. pAS2 plasmids containing single-residue substitutions of the FHA1 pThr-binding site were described before (36). Additional constructs were generated by PCR and cloned into pGADGH, and correct sequences were confirmed by cDNA sequence analysis.

Cell cycle analyses. Cells were synchronized by treatment of log-phase cultures with 15 μg of nocodazole (Calbiochem)/ml for 90 min plus another 10 μg/ml for 60 min or by treatment with two doses of 20 μg of α-factor/ml over 3 h. Synchrony (>90%) was assessed by microscopy. For MMS checkpoint experiments, cells were treated with 0.05% MMS for the last 30 min of the nocodazole arrest and washed with and released into YPD containing 0.05% MMS. For UV experiments, cells were irradiated with 80 J/m^2 and released into YPD after three washes. Aliquots were fixed in 70% ethanol and stained with 4′,6′-diamidino-2-phenylindole (DAPI), and ≥100 cells were scored per sample at a magnification of ×400 with a Zeiss Axiovert 25 inverted phase-contrast and fluorescence microscope (37). Flow cytometry analyses were performed as described previously (36).

Immunofluorescence microscopy. Five-milliliter cultures were grown to 1 × 10^7 to 2 × 10^7 cells/ml, initially fixed with 3.7% formaldehyde for 10 min, and resuspended in PEM buffer (100 mM PIPES, 1 mM EGTA, 1 mM $MgSO_4$ [pH 6.9]) containing 3.7% formaldehyde for overnight fixation at 4°C. Cells were washed twice with PEM buffer, incubated with 150 mM glycine in phosphate-buffered saline (PBS) for 10 min, washed with PEMS (PEM buffer, 1.2 M sorbitol), resuspended in 1 ml of PEMS containing 0.25 mg of Zymolyase 20T (Seikagaku), and incubated at 30°C for 10 to 30 min until cell walls were digested. Cells were immediately placed on ice, washed with PEMS, and resuspended in 0.5 ml of PEMS. Cell suspensions (20 μl) were dried on polylysine-coated slides, washed twice with PBS, and submerged in −20°C methanol for 6 min and −20°C acetone for 30 s. Slides were washed twice with PBS and blocked with PBS-T-B (PBS, 0.1% Tween 20, 1% bovine serum albumin) for 1 h in a humid chamber. Primary antibody incubation with 1/100-diluted antitubulin TAT1 (generously provided by Matthew O'Connell) in PBS-T-B was performed overnight at 4°C, followed by four PBS–0.1% Tween 20 (PBS-T) washes at room temperature. Alexa 594-conjugated goat anti-mouse immunoglobulin G (Molecular Probes) in PBS-T-B was added at room temperature. After 1 h, DNA was counterstained with 1.7 μg of Hoechst 33258/ml in PBS-T for 10 min, and slides were washed four times with PBS-T. Coverslips were mounted with fluorescence microscopy

mounting medium (Dako) and sealed with nail polish. Photomicrographs were taken on Kodak 320-T color reversal film at an original magnification of ×250 by using a 100× oil immersion objective.

Protein blots, kinase assays, and immunoprecipitation. Immunoblotting was performed as previously described (36, 37). For immunoprecipitation, clarified yeast extracts were prepared with native lysis buffer (PBS containing 10% glycerol, 1% NP-40, 0.5% Triton X-100, 5 mM EDTA, 5 mM EGTA, 50 NaF, 10 mM β-glycerophosphate, 5 mM sodium pyrophosphate, 2 mM phenylmethylsulfonyl fluoride, and 1× protease inhibitor mix [Sigma]) by bashing with glass beads and were incubated for 2 h at 4°C with 20 μg of mouse anti-myc monoclonal antibody 9E10 (generously provided by Andy Poumbourios)/ml and 20 μl of protein G-Sepharose (Amersham), washed with lysis buffer, and eluted into sodium dodecyl sulfate loading buffer. Rabbit polyclonal anti-pThr antibody was obtained from Cell Signaling, and mouse monoclonal antiactin antibody was obtained from Chemicon.

Kinase assays were carried out as described previously (20) for 20 min at 30°C in a 20-μl reaction mixture containing 20 mM Tris (pH 7.4), 10 mM magnesium acetate, 4 mM manganese chloride, 0.1 mM dithiothreitol, 0.05% (wt/vol) Tween 20, 50 μM ATP, and 1 μCi of [γ-^{32}P]ATP with anti-myc antibody immunoprecipitates from 10-ml log-phase cultures treated with 0.05% MMS. A recombinant Mdt1 (positions 531 to 668)-His$_6$ fragment was purified by Ni^{2+}-agarose chromatography essentially as described previously (19) and added at ~20 ng/μl. Reactions were stopped by boiling in sample buffer, and 15 μl from a 40-μl total volume was analyzed by sodium dodecyl sulfate-polyacrylamide gel electrophoresis and autoradiography.

RESULTS

Identification of Mdt1 as a Rad53 FHA1 domain-interacting protein. In order to identify novel Rad53 FHA1-binding proteins, a yeast two-hybrid screen of a yeast cDNA library fused to the Gal4 AD was performed with a Gal4 BD-FHA1 domain fusion vector as bait. In this system, protein-protein interactions of AD-containing and BD-containing fusion proteins in cotransformed yeast cells restore Gal4 transcriptional activity and lead to the expression of *HIS3* and *ADE2* reporter genes from distinct promoters, allowing growth on plates lacking both histidine and adenine (16). This approach led to the isolation of an FHA1-interacting clone expressing an in-frame AD fusion protein with residues 302 to 668 encoded by the previously uncharacterized yeast open reading frame *YBL051C*, which we have termed *MDT1* (Fig. 1). Full-length Mdt1 contains 668 residues, with an N-terminal RNA recognition motif (RRM) domain, a nuclear localization signal, a coiled coil, and a total of 15 SQ/TQ motifs; 14 of the latter motifs are concentrated within 288 residues, including a 60-residue supercluster containing 1 TQ motif and 8 SQ motifs (Fig. 1A). Such SQ/TQ cluster domains (SCDs), which represent potential phosphorylation sites for ATM-like kinases, are a hallmark of numerous checkpoint proteins, including Rad53, Rad9, and Mrc1 (2, 26, 42); the Rad9 SCD (containing six SQ/TQ motifs between residues T390 and Q458) was recently shown to be critical for the interaction with Rad53 (42).

Interestingly, the FHA1-Mdt1 interaction was abolished by several single-residue substitutions that disrupt the FHA1 phosphopeptide-binding site (36), including the very subtle R70K and S105T substitutions (Fig. 1B); this result indicates that Mdt1 interacts specifically with the pThr-binding site of the Rad53 FHA1 domain. Truncation analyses revealed that residues 297 to 375 of the Mdt1 SCD are sufficient and critical for its interaction with the FHA1 domain, as their deletion abolished reporter gene activation, whereas the C-terminal SQ/TQ motif supercluster was dispensable for this interaction (Fig. 1C). Importantly, substitution of the single Thr residue

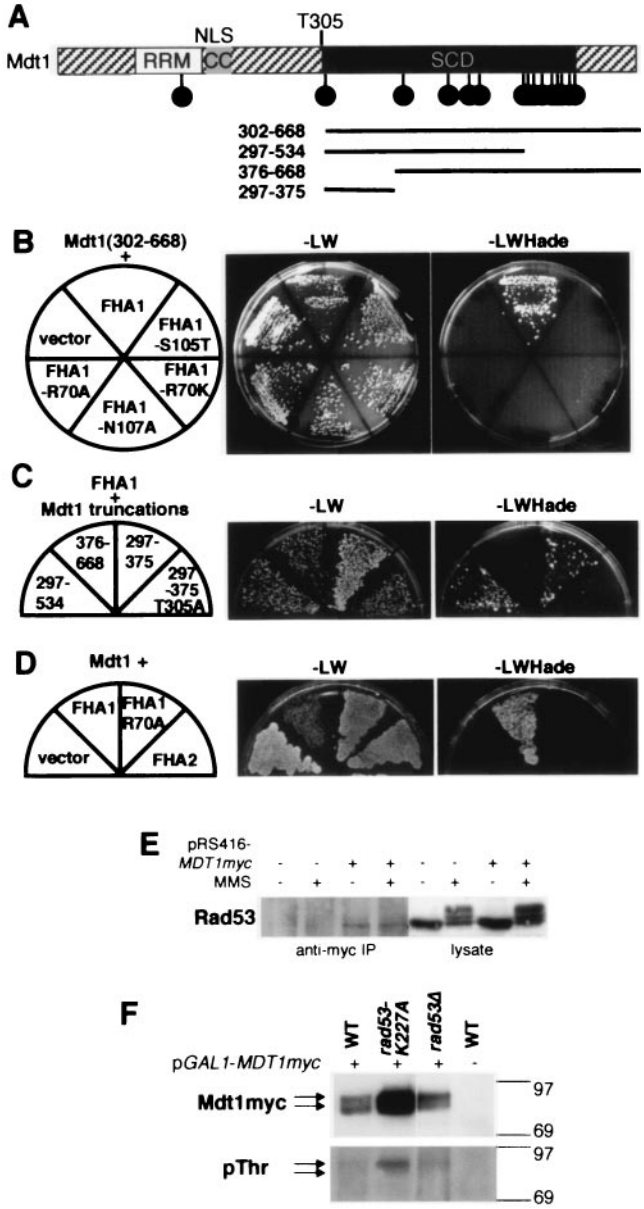

FIG. 1. Mdt1 interaction with the Rad53 FHA1 domain. (A) Schematic diagram of Mdt1 domain topology and positions of SQ/TQ motifs (balls). Bars and numbers indicate Mdt1 fragments used in interaction assays. NLS, nuclear localization signal; CC, coiled coil. (B to D) Yeast two-hybrid analysis of Mdt1 (positions 302 to 668) with a wild-type or mutated FHA1 domain or an empty vector (B), of the indicated Mdt1 fragments with a wild-type FHA1 domain (C), or of pGADGH-*MDT1* with the FHA1 and FHA2 domains (D). Cotransformed cultures were streaked on plates lacking Leu and Trp (−LW) or lacking Leu, Trp, His, and Ade but containing 10 mM 3-amino-1,2,4-triazole (−LWHade). (E) Rad53 Western blot of anti-myc antibody immunoprecipitates (IP) from the indicated cultures (four left lanes) and the corresponding lysates (3% of input; four right lanes) without or with MMS treatment. (F) Western blot analysis of immunoprecipitated myc-tagged Mdt1 expressed from the *GAL1* promoter in the indicated strains probed with anti-myc antibody (top panel) or reprobed with anti-pThr antibody (bottom panel). Arrows indicate the positions of the myc-tagged Mdt1 bands. Numbers at right indicate mass standards (kilodaltons). WT, wild type.

(T305) of the Mdt1 fragment from residues 297 to 375 by Ala inhibited its interaction with the FHA1 domain (Fig. 1C). In contrast to its interaction with the Rad53 FHA1 domain, Mdt1 did not interact with the Rad53 FHA2 domain (Fig. 1D). The reciprocal dependence of the Rad53 FHA1 domain-Mdt1 interaction on the integrity of the FHA1 pThr-binding site and the presence of T305 in Mdt1 strongly indicates that Mdt1 interacts with Rad53 in a pThr-specific manner.

Constitutive Mdt1 phosphorylation and Rad53 interaction in vivo. Small amounts of Rad53 could be coimmunoprecipitated with an anti-myc antibody from a yeast strain expressing myc-tagged Mdt1 at essentially physiological levels (under the control of its own promoter on a low-copy-number centromeric plasmid in an *mdt1*Δ strain) but not from the wild-type strain expressing untagged Mdt1, confirming the two-hybrid interaction of the two proteins (Fig. 1E). The myc tag did not interfere with Mdt1 function (see Fig. 5B). Surprisingly, this interaction had already occurred in the absence of MMS treatment and seemed to involve predominantly unphosphorylated or underphosphorylated Rad53 (Fig. 1E). However, immunoprecipitated myc-tagged Mdt1 consistently appeared as a doublet in Western blots, and the more slowly migrating Mdt1 form already reacted with an anti-pThr antibody under basal conditions (Fig. 1F). Together with the results of the two-hybrid analysis, these data suggest that Mdt1 is constitutively phosphorylated on Thr as a prerequisite for its interaction with the Rad53 FHA1 domain.

Mec1/Tel1-dependent Mdt1 hyperphosphorylation in response to DNA damage. For unknown reasons, we found highly variable levels of expression of myc-tagged Mdt1 from plasmid vectors in various checkpoint mutants (for example, note the higher levels of plasmid-expressed myc-tagged Mdt1 in *rad53-K227A*; Fig. 1F). As this fact complicated Mdt1 phosphorylation analysis after DNA damage, we generated a stable *MDT1-myc* allele by integrating a C-terminal myc tag into the genomic *MDT1* locus, resulting in essentially equal protein levels in all strains tested (Fig. 2 and data not shown). Interestingly, Mdt1 was shifted to more slowly migrating forms in response to MMS treatment (Fig. 2A). This DNA damage-dependent hypershift (as well as the constitutive pThr shift) could be reversed by pretreatment of immunoprecipitated myc-tagged Mdt1 with λ phosphatase (Fig. 2B), indicating that Mdt1 is hyperphosphorylated in response to DNA damage.

Mdt1 was still noticeably hypershifted after DNA damage in *mec1*Δ cells (Fig. 2A, bottom panel) as well as in *rad53*Δ and *chk1*Δ cells (data not shown). *S. cerevisiae* contains a second ATM-like kinase, Tel1, which has an overlapping substrate specificity and can sometimes substitute for Mec1 (14, 30, 49). We therefore generated a *mec1*Δ *tel1*Δ double-deletion strain to test whether the DNA damage-dependent Mdt1 hyperphosphorylation is checkpoint dependent. Importantly, MMS-induced Mdt1 hyperphosphorylation was essentially abolished in the *mec1*Δ *tel1*Δ strain (Fig. 2C), demonstrating that Mdt1 is a checkpoint target. Furthermore, a recombinant Mdt1 fragment containing the supercluster of nine SQ/TQ motifs was readily phosphorylated in myc immunoprecipitates from a strain containing a myc-tagged *MEC1* allele but not from the untagged wild-type strain (Fig. 2D). Although we cannot exclude the possibility that the Mec1 immunoprecipitates contained another Mec1-associated protein kinase, this experiment strongly suggests that Mdt1 is a direct Mec1 kinase substrate. Altogether, these experiments indicate that Mdt1 is an in vivo substrate of the yeast ATM-like kinase Mec1/Tel1.

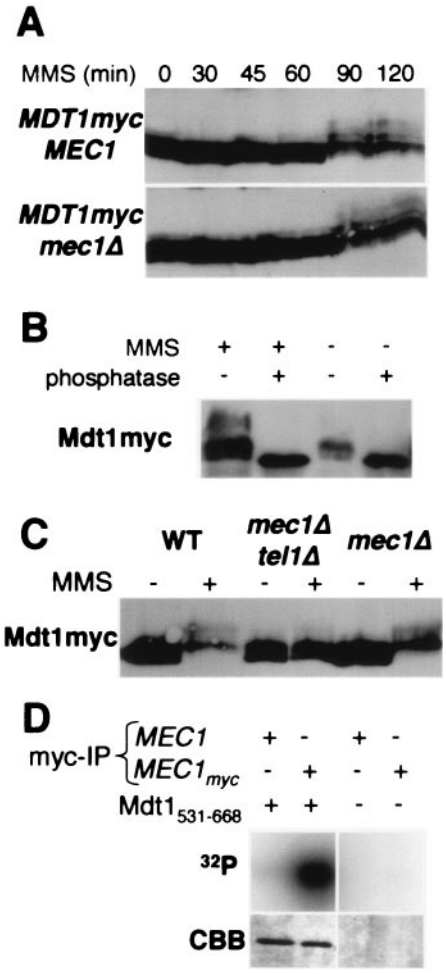

FIG. 2. DNA damage-dependent Mdt1 hyperphosphorylation. (A) Anti-myc antibody Western blot analysis of chromosomally myc-tagged Mdt1 in wild-type (top) and *mec1*Δ (bottom) cells treated with 0.1% MMS for the indicated times. (B) Western blot of immunoprecipitated myc-tagged Mdt1 expressed from a centromeric plasmid under the control of its own promoter in *mdt1*Δ cells in the presence or absence of 0.1% MMS. Some samples were incubated with λ phosphatase before electrophoresis. (C) Anti-myc antibody Western blot analysis of chromosomally myc-tagged Mdt1 without or with 0.1% MMS treatment for 2 h in wild type, *mec1*Δ, and *mec1*Δ *tel1*Δ cells. (D) Kinase assays of myc-tagged Mec1 or control immunoprecipitates (IP). The left panels show kinase reactions with Mdt1 (positions 531 to 668) as a substrate; the right panels show no-substrate controls of the corresponding gel areas. Phosphorimaging autoradiographs are shown in the top panels; the relevant sections of the gels stained with Coomassie brilliant blue (CBB) are shown in the bottom panels.

Genetic interactions of *MDT1* with checkpoint components. To further evaluate the roles of *MDT1* in DNA damage, we tested *MDT1* for genetic interactions with other checkpoint genes. *MDT1* showed a strong genetic interaction with *rad53*Δ in overexpression experiments with a p*GAL1-MDT1-myc* plasmid compared to the empty vector control on medium containing 4% galactose. Under these conditions, *MDT1* overexpression had no effect on wild-type cells but reduced colony

formation of *rad53*Δ cells in the absence of exogenous DNA-damaging agents by ~100-fold (Fig. 3A). Because *rad53*Δ cells are severely compromised in checkpoint functions and are kept viable only by higher deoxynucleoside triphosphate levels resulting from the *sml1*Δ mutation (51, 52), these data suggest that elevated Mdt1 levels hypersensitize *rad53*Δ mutants to endogenous DNA damage.

We next tested whether *mdt1*Δ affects DNA damage sensitivity by treating liquid cultures with 0.04% MMS for 3 h. In these assays, *mdt1*Δ generally improved DNA damage tolerance, even in the wild-type strain, and was particularly efficient in suppressing the DNA damage hypersensitivity of checkpoint-compromised *rad9*Δ and *rad17*Δ strains, resulting in a four- to fivefold increase in viability (Fig. 3B). The *mdt1*Δ effect was even more dramatic in a *rad9*Δ *rad53-R70A* double-mutant background. *rad9*Δ *rad53-R70A* were considerably more hypersensitive to MMS than either single mutation (Fig. 3C), but this hypersensitivity was completely suppressed by *mdt1*Δ, resulting in ~100-fold more efficient colony formation (Fig. 3C, compare lanes 6 and 8). However, *mdt1*Δ had no effect on *rad53*Δ, indicating that it acts in a Rad53-dependent manner. Altogether, these various genetic interactions of *MDT1* (Fig. 3) are consistent with its direct interaction with Rad53 (Fig. 1) and its Mec1/Tel1-dependent phosphorylation after DNA damage (Fig. 2) and strongly support its connection with the checkpoint machinery.

Role of Mdt1 in the normal G_2/M transition and DNA damage-dependent cell cycle delay. A major reason for the DNA damage hypersensitivity of *rad9*Δ and *rad17*Δ strains is their inability to delay anaphase in response to DNA damage (50). We therefore investigated the role of *MDT1* in G_2/M cell cycle transitions by scoring nuclear division kinetics after the release of cells from nocodazole arrest. Interestingly, under control conditions, the completion of mitosis after nocodazole release was delayed by about 20 min in *mdt1*Δ cells compared to wild-type cells (Fig. 4A), with a much lower content of binucleate cells (wild type, 40.2% ± 3.2%; *mdt1*Δ, 28% ± 3.6%) after 60 min. Similar results were obtained for several checkpoint-deficient strains, where the *mdt1*Δ allele consistently caused delayed binucleation kinetics compared to the relevant *MDT1* control (Fig. 4A and data not shown). For all of these strains, *mdt1*Δ cultures (in rich media, irrespective of DNA-damaging agents) contained a considerable number of cells with aberrant morphology. *mdt1*Δ cells appeared elongated and multibudded, both in mononucleated premitotic cells (Fig. 5A) and in binucleated postmitotic cells (Fig. 5A); as a consequence, mitotic spindles in *mdt1*Δ cells were considerably longer than those in the corresponding wild-type cells (Fig. 5A, bottom panel). The aberrant morphology was reversed by the expression of *MDT1-myc* under the control of its own promoter on a centromeric plasmid (Fig. 5B). This *mdt1*Δ phenotype is reminiscent of that of cell cycle mutants that maintain high levels of G_1 cyclin-dependent kinase activity (Cdc28-Cln) but insufficient levels of G_2/M cyclin-dependent kinase activity (Cdc28-Clb) required for switching from apical to isotropic bud growth during G_2/M phase, for example, mutations in *CLB1/2* (47), *CDC34* (44), or *FKH1/2* forkhead transcription factors (25). Therefore, the aberrant morphology of *mdt1*Δ cells (Fig. 5A) and their delayed binucleation kinetics after release from nocodazole arrest in the absence of exogenous

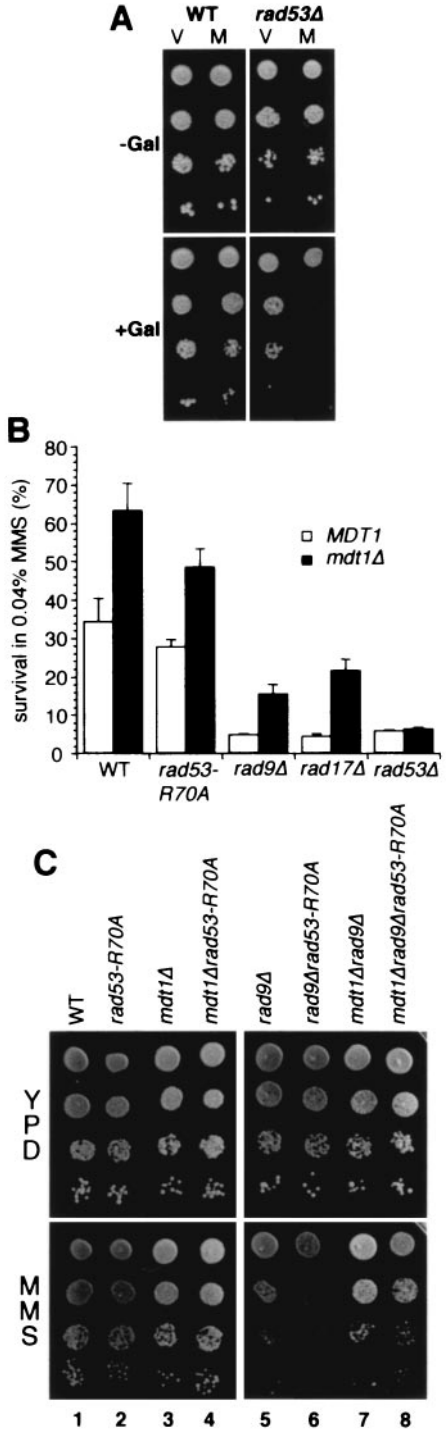

FIG. 3. Genetic interactions of *MDT1* with checkpoint components. (A) Drop test analysis of serial 10-fold dilutions of the indicated yeast strains transformed with p*GAL1-MDT1-myc* (M) or an empty vector control (V) plated on medium lacking uracil but containing 2% sucrose (−Gal) or 2% sucrose and 4% galactose (+Gal). WT, wild type. (B) Survival analysis of the indicated yeast strains treated with 0.04% MMS for 3 h. Data are the mean and standard error of three experiments. (C) Drop test analysis of serial 10-fold dilutions of the indicated yeast strains on YPD (top panels) or YPD containing 0.02% MMS (bottom panels).

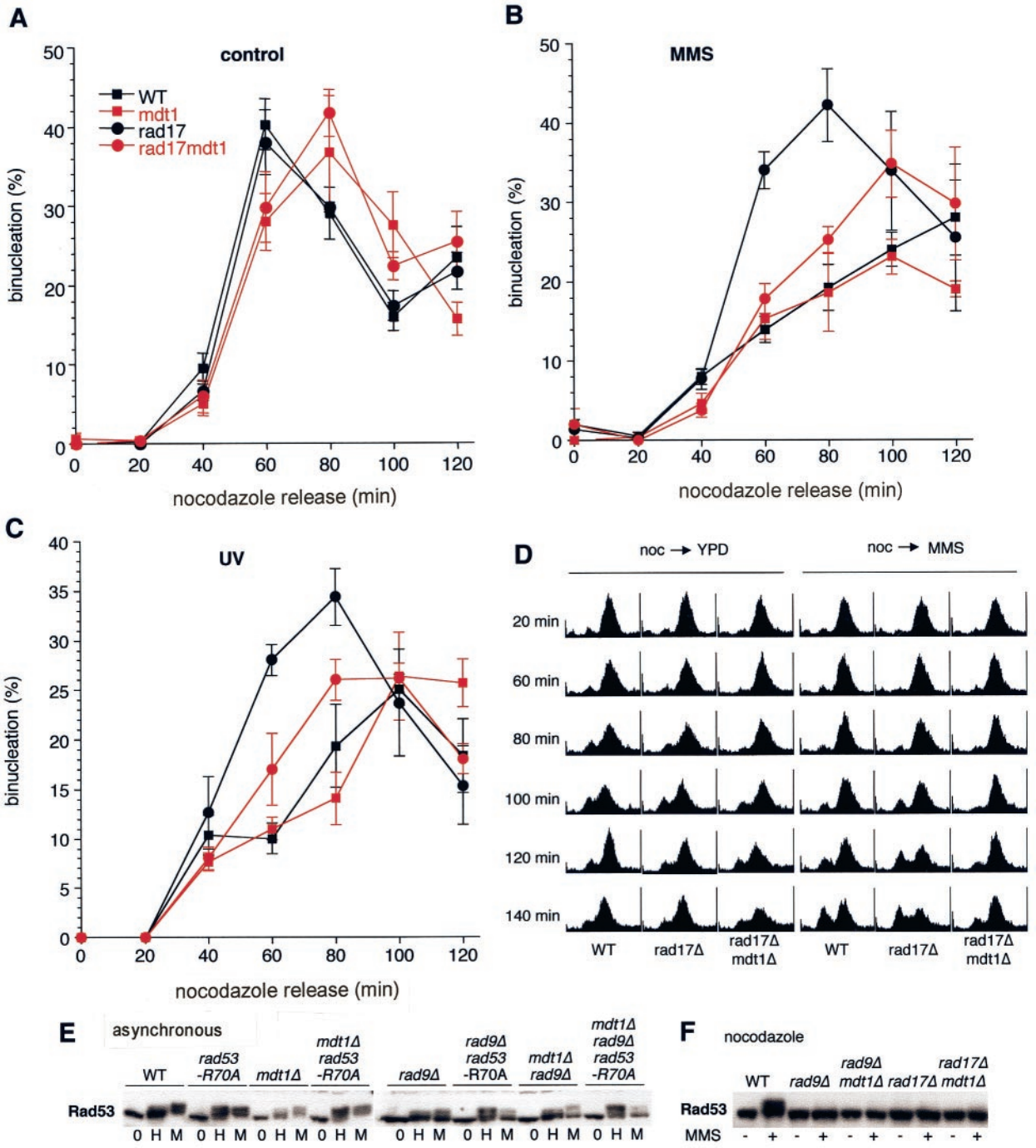

FIG. 4. Role of *MDT1* in G_2/M cell cycle progression. (A to C) Percentages of binucleated cells (mean and standard error of ≥3 independent experiments) in the indicated strains after release from nocodazole arrest under control conditions (A) and in response to MMS (B) and UV (C) damage. (D) Flow cytometry analysis of similar samples. The main peak at 20 min represents G_2/M cells with a 2n DNA content; the peak with a 1n DNA content at later time points represents G_1 cells. noc, nocodazole; WT, wild type. (E and F) Western blot analyses of Rad53 in the indicated strains from untreated cultures (0) (E), from unsynchronized cultures treated with 150 mM HU (H) or 0.1% MMS (M) for 1 h (E), or from nocodazole-arrested cultures without or with 0.1% MMS treatment (F).

DNA damage (Fig. 4A) indicate that Mdt1 has a physiological function in contributing to the G_2/M transition during normal cell cycles.

We next tested how the delayed binucleation kinetics of *mdt1*Δ cells were affected by DNA damage of cells prior to the nocodazole release. As expected, wild-type cells had significantly delayed binucleation kinetics after pretreatment with MMS (Fig. 4B) or UV (Fig. 4C), in contrast to *rad17*Δ cells, which showed barely delayed progression through mitosis. Interestingly, in response to DNA damage, *mdt1*Δ cells had binucleation kinetics very similar to those of wild-type cells, in contrast to their delayed kinetics under control conditions. If

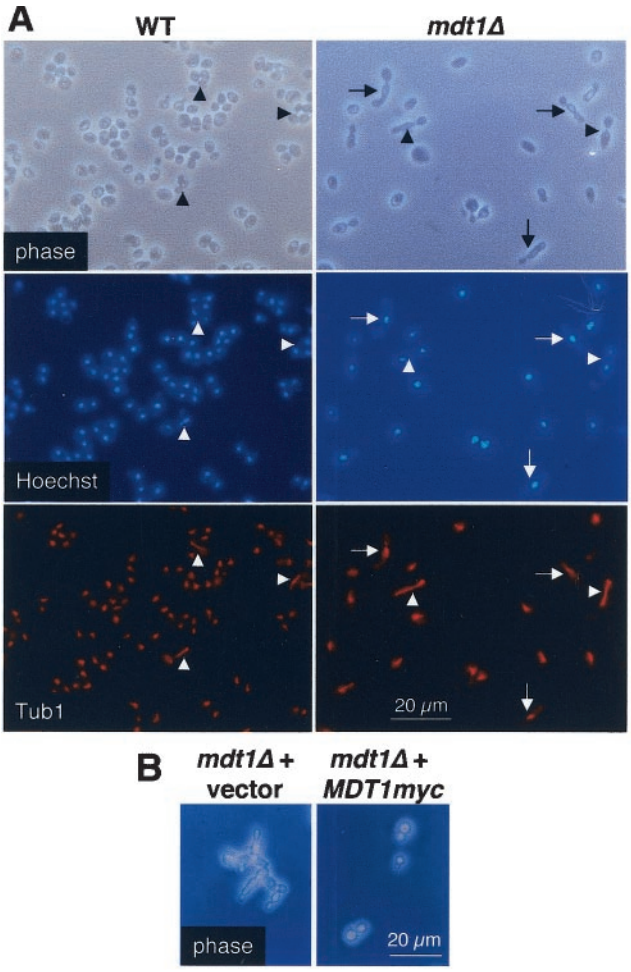

FIG. 5. Aberrant morphology of *mdt1*Δ cells. (A) Phase-contrast and fluorescence photomicrographs of *MDT1* (WT) or *mdt1*Δ cells grown in YPD without DNA-damaging agents and stained for nuclear DNA (Hoechst) and tubulin. (B) Phase-contrast micrographs of *mdt1*Δ cells containing pRS416 or pRS416-*MDT1-myc*.

DNA damage-dependent and *mdt1*Δ-dependent cell cycle delays are independent, then *mdt1*Δ cells should progress more slowly through mitosis than wild-type cells irrespective of damage; however, in response to MMS they had essentially identical nuclear division kinetics (Fig. 4B). Thus, the finding that *mdt1*Δ-dependent and DNA damage-dependent cell cycle delays are not additive suggests that they are epistatic, genetically placing them in the same pathway.

The *mdt1*Δ-dependent delay was fully maintained and even enhanced in response to DNA damage in the *rad17*Δ *mdt1*Δ strain compared to the parental *rad17*Δ strain, in a manner that almost approached the checkpoint-induced delay in wild-type cells (Fig. 4B and C). Similar results were obtained for other checkpoint mutants carrying the *mdt1*Δ allele (*rad9*Δ *mdt1*Δ and *lcd1*Δ *mdt1*Δ; data not shown) and were confirmed in flow cytometry experiments, where the reemergence of G_1 cells (with a 1n DNA content) was not delayed by MMS treatment in *rad17*Δ cells but was delayed by ~40 min in wild-type cells and by more than 20 min in *rad17*Δ *mdt1*Δ cells (Fig. 4D). Because such delays would allow more time for DNA damage repair, these results provide an explanation for the DNA damage-protective effect of *mdt1*Δ (Fig. 3).

*mdt1*Δ had no effect on Rad53 activation for the various strains analyzed in asynchronous (Fig. 4E and data not shown) or nocodazole-arrested (Fig. 4F) cultures, indicating that the delayed cell cycle kinetics are not a consequence of restored Rad53 activation. These results suggest that Mdt1 acts downstream of or in parallel with Rad53.

Because residue T305 is critical for the interaction of Mdt1 with the Rad53 FHA1 domain (Fig. 1C), we generated an *mdt1-T305A* allele to test its role in the DNA damage response. This allele did not obviously affect DNA damage sensitivity in an otherwise wild-type background but, interestingly, led to slightly but reproducibly reduced hypersensitivity to MMS and UV in *rad17*Δ cells (Fig. 6), similar to *mdt1*Δ. These results indicate that T305 does not function solely to target Mdt1 to the checkpoint machinery via the Rad53 FHA1 domain, in which case it would be expected to result in damage hypersensitivity similar to that of the *rad53-R70A* allele, but rather that it has additional functions in cell cycle control or the DNA damage response.

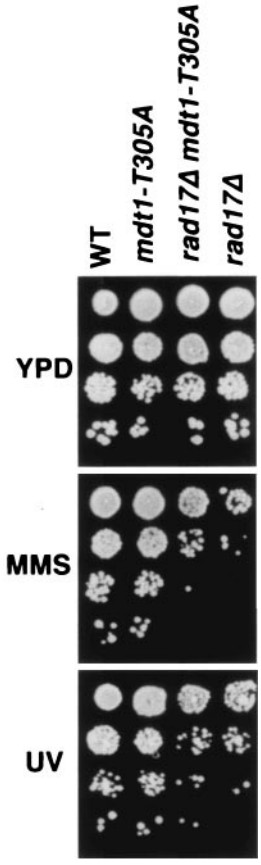

FIG. 6. Partial suppression of *rad17*Δ DNA damage hypersensitivity by *mdt1-T305A*. Equal serial 10-fold dilutions of the indicated strains (starting optical density at 600 nm, ~0.5) were spotted on control plates after being untreated (top) or treated for 3 h with 0.04% MMS (middle) or 150 J of UV light per m^2 (bottom). WT, wild type.

DISCUSSION

Cell cycle function of Mdt1. In this study, we have identified Mdt1 as a novel protein involved in G_2/M progression during normal cell cycles as well as the cellular response to DNA damage. *mdt1*Δ cells are delayed in completing mitosis after release from a preanaphase arrest (Fig. 4A) and have a morphological phenotype characteristic of G_2/M cell cycle mutants (Fig. 5A), indicating that Mdt1 normally promotes progression through late phases of the cell cycle. The mechanism of Mdt1 function during normal cell cycles is currently unclear. In BLAST searches, the highest scores are restricted to the Mdt1 RRM domain, which is remarkably similar to RRM domains in two uncharacterized putative fission yeast proteins (on cosmids SPAC12G12 and SPBC16A3; >60% identity and ≥80% similarity) and reasonably similar to an RRM domain in mammalian mRNA cleavage-stimulating factors (31% identity and 51% similarity). Mdt1 therefore could have a function in RNA metabolism, possibly in the posttranscriptional regulation of genes involved in G_2/M cell cycle progression. However, RRM domains are not restricted to protein-RNA interactions, as some RRM domains mediate interactions with single-stranded DNA, for example, in the yeast telomeric DNA-binding protein Gbp2 (29) (30% RRM identity with Mdt1); these data could be relevant for interactions with single-stranded DNA resulting from the processing of DNA double-strand breaks. Interestingly, a novel human protein termed ASCIZ, which shares remarkable structural and functional similarities with Mdt1, was recently identified (C. J. McNees et al., unpublished data). The two proteins have similar domain topologies, with an N-terminal nucleic acid-binding domain (a double Zn^{2+} finger domain in ASCIZ instead of an RRM domain) followed by a nuclear localization signal and a C-terminal SCD, and a high level of sequence similarity (>17% identity and >36% strong similarity). Like Mdt1, ASCIZ interacts via its SCD with the pThr-binding site of the FHA domain of the human Rad53 ortholog Chk2, and it has roles during normal cell cycles and in the DNA damage response. These data indicate that Mdt1 and ASCIZ are the founding members of an evolutionarily conserved protein family.

While this work was in progress, *MDT1* (*YBL051C*) was independently isolated in three unrelated genetic screens. In an automated high-throughput screen, *mdt1*Δ was found to be synthetic lethal with *bni1*Δ, involved in actin cable assembly, polarized cell growth, and preanaphase spindle orientation (48). Interestingly, while *MDT1* or the mechanism of its genetic interaction with *BNI1* was not further characterized, several other synthetically lethal interactions of *bni1*Δ in this screen involved genes functioning in mitosis and the transition from apical to isotropic bud growth (48); these data indirectly support our conclusion of a cell cycle function for Mdt1. Likewise, in a systematic analysis of cell size distribution in all available gene deletion strains, an *mdt1*Δ strain was found to be among the 5% most abnormally large strains (23), consistent with our morphological findings (Fig. 5). In another study, *YBL051C* was designated *PIN4* because it is present on a plasmid that can induce prion formation in yeast cells when overexpressed at very high levels (10). However, it is unclear whether *YBL051C* is indeed responsible for the PIN^+ phenotype, first because *YBL051C* was significantly truncated on the *PIN4* plasmid and second because it was not the only open reading frame on this plasmid (10).

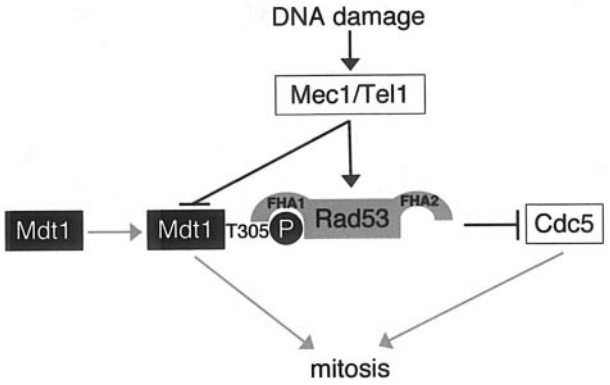

FIG. 7. Model for the role of Mdt1 during normal cell cycles (grey lines) and in response to DNA damage (black lines). Mdt1 phosphorylation on T305 contributes to normal mitosis in unperturbed cell cycles, in a pathway parallel to that of Cdc5. Phosphorylated T305 also functions as a scaffold to link Mdt1 to the checkpoint machinery via the interaction of Mdt1 with the Rad53 FHA1 domain pThr-binding site. In response to DNA damage, Mdt1 is phosphorylated on multiple residues in a Mec1/Tel1-dependent manner, inhibiting its promitotic function. Together with checkpoint-dependent inactivation of parallel pathways, for example, Rad53-dependent phosphorylation of Cdc5, this event leads to G_2/M delays while DNA damage persists.

Mdt1 functions as a checkpoint target. The following considerations strongly support the notion that Mdt1 is a novel checkpoint target. First, Mdt1 interacts physically with the Rad53 FHA1 domain, linking it to the checkpoint machinery (Fig. 1). Second, Mdt1 hyperphosphorylation in response to DNA damage in vivo is checkpoint dependent, and Mdt1 is a direct Mec1 kinase substrate in vitro (Fig. 2). Third, *MDT1* exhibits several strong genetic interactions with other checkpoint components (Fig. 3).

Checkpoint-dependent phosphorylation either can activate targets to fulfill their DNA damage response functions, for example, Rad9 (49), Rad53 (40), or Rad55 (3), or can inhibit protein functions that antagonize the DNA damage response, for example, Sml1 (51) or Dbf4 (11). Given that the promitotic function of Mdt1 is intrinsically antagonistic to cell cycle arrest checkpoints, the most plausible explanation for Mec1/Tel1-dependent phosphorylation is that it serves to negatively regulate Mdt1 functions in order to facilitate cell cycle arrest in the presence of DNA damage (Fig. 7). This model is supported by the finding that the *mdt1*Δ-dependent and DNA damage-induced cell cycle delays are not additive (Fig. 4B), suggesting that both act in the same pathway. Because the negative regulation of Mdt1 functions by checkpoints would have the same effect as the deletion of Mdt1, we propose that the partial restoration of the G_2/M checkpoint in *rad17*Δ cells by *mdt1*Δ is not simply an indirect consequence of slower mitosis in the absence of Mdt1 but rather indicates that Mdt1 is an important downstream target of cell cycle arrest checkpoints. The fact that *mdt1*Δ does not fully restore the G_2/M arrest checkpoint in *rad17*Δ cells could be explained by the presence of parallel pathways, for example, the well-established Cdc5–anaphase-promoting complex pathway (39) (Fig. 7).

Our data establish Mdt1 as a member of a growing list of proposed Rad53 FHA1 domain ligands that includes Rad9

(13), Dbf4 (11), Asf1 (43), and Ptc2/3 (27), highlighting the versatility of this pThr-binding domain. Rad53 interacts with Mdt1 even in the absence of DNA damage, a finding which is most likely due to the fact that the critical Mdt1 residue, T305, is partially phosphorylated during normal cell cycles (Fig. 1). At this point, it remains to be determined whether the phosphorylated T305-FHA1 interaction functions to link Mdt1 to the checkpoint machinery in general (Fig. 7) or whether it facilitates a direct kinase-substrate interaction with Rad53. Mdt1 hyperphosphorylation in response to DNA damage results in a heterogeneous electrophoretic mobility pattern similar to those of other SCD-containing proteins, such as Rad9 (42), Rad53 (37), and Mrc1 (2). These data indicate that multiple sites are phosphorylated to variable degrees, reminiscent of the cell cycle-dependent phosphorylation of Sic1, where the biological effect depends not so much on the precise location of phosphorylation sites but rather on a threshold of a minimal number of phosphorylated residues (33). Mdt1 contains 15 SQ/TQ motifs, and our in vivo and in vitro data (Fig. 2) indicate that Mec1 and Tel1 are the major Mdt1 kinases. DNA damage-dependent Mdt1 phosphorylation was apparently unaffected in *rad53*Δ cells (data not shown), but a limited number of Rad53-specific phosphorylation events would be obscured easily by the heterogeneous banding pattern resulting from multiple Mec1/Tel1 phosphorylation sites. However, T305 seems to have additional functions beyond its role in linking Mdt1 to the checkpoint machinery, because the *mdt1-T305A* allele paradoxically acted as a partial suppressor of *rad17*Δ-associated DNA damage hypersensitivity (Fig. 6), similar to *mdt1*Δ. The simplest explanation for this observation is that the basal phosphorylation of T305 contributes to the normal cell cycle function of Mdt1 (Fig. 7), such that its replacement by nonphosphorylatable A305 results in an *mdt1*Δ-like DNA damage phenotype. This dual function of phosphorylated T305 could serve as a "go" signal during unperturbed cell cycles but at the same time provide an immediate target for "stop" signals in response to DNA damage by linking Mdt1 to the Mec1/Tel1 pathway.

In conclusion, we have identified Mdt1 as a novel protein involved in G_2/M cell cycle progression and as a novel checkpoint target. The results provide the basis for future studies of the precise mechanisms of Mdt1 functions during normal cell cycles and Mdt1 regulation by and roles in DNA damage checkpoints.

ACKNOWLEDGMENTS

We thank Nora Tenis for help with recombinant protein expression; Catherine Dale for help in generating some of the yeast strains; Tony Tiganis for help with FACS analyses; Lena Burri for help with tetrad dissections; Rodney Rothstein, Stephen Jackson, Matthew O'Connell, and Andy Poumbourios for strains and antibodies; and members of our laboratories, Steve Dalton, and Anton Gartner for discussions and comments on the manuscript.

This work was supported by grants from the National Health and Medical Research Council of Australia (NHMRC) and the Cancer Council of Victoria (to J.H.), National Institutes of Health grant CA87031 (to M.-D.T.), an Australian postgraduate award (to B.L.P.), and an NHMRC senior research fellowship (to J.H.).

REFERENCES

1. **Abraham, R. T.** 2001. Cell cycle checkpoint signaling through the ATM and ATR kinases. Genes Dev. **15:**2177–2196.
2. **Alcasabas, A. A., A. J. Osborn, J. Bachant, F. Hu, P. J. Werler, K. Bousset, K. Furuya, J. F. Diffley, A. M. Carr, and S. J. Elledge.** 2001. Mrc1 transduces signals of DNA replication stress to activate Rad53. Nat. Cell Biol. **3:**958–965.
3. **Bashkirov, V. I., J. S. King, E. V. Bashkirova, J. Schmuckli-Maurer, and W. D. Heyer.** 2000. DNA repair protein Rad55 is a terminal substrate of the DNA damage checkpoints. Mol. Cell. Biol. **20:**4393–4404.
4. **Bell, D. W., J. M. Varley, T. E. Szydlo, D. H. Kang, D. C. Wahrer, K. E. Shannon, M. Lubratovich, S. J. Verselis, K. J. Isselbacher, J. F. Fraumeni, J. M. Birch, F. P. Li, J. E. Garber, and D. A. Haber.** 1999. Heterozygous germ line hCHK2 mutations in Li-Fraumeni syndrome. Science **286:**2528–2531.
5. **Burke, D., D. Dawson, and T. Stearns.** 2000. Methods in yeast genetics. Cold Spring Harbor Laboratory Press, Cold Spring Harbor, N.Y.
6. **Carney, J. P., R. S. Maser, H. Olivares, E. M. Davis, M. Le Beau, J. R. Yates III, L. Hays, W. F. Morgan, and J. H. Petrini.** 1998. The hMre11/hRad50 protein complex and Nijmegen breakage syndrome: linkage of double-strand break repair to the cellular DNA damage response. Cell **93:**477–486.
7. **Clerici, M., V. Paciotti, V. Baldo, M. Romano, G. Lucchini, and M. P. Longhese.** 2001. Hyperactivation of the yeast DNA damage checkpoint by TEL1 and DDC2 overexpression. EMBO J. **20:**6485–6498.
8. **Cortez, D., S. Guntuku, J. Qin, and S. J. Elledge.** 2001. ATR and ATRIP: partners in checkpoint signaling. Science **294:**1713–1716.
9. **de la Torre-Ruiz, M. A., C. M. Green, and N. F. Lowndes.** 1998. RAD9 and RAD24 define two additive, interacting branches of the DNA damage checkpoint pathway in budding yeast normally required for Rad53 modification and activation. EMBO J. **17:**2687–2698.
10. **Derkatch, I. L., M. E. Bradley, J. Y. Hong, and S. W. Liebman.** 2001. Prions affect the appearance of other prions: the story of [PIN+]. Cell **106:**171–182.
11. **Duncker, B. P., K. Shimada, M. Tsai-Pflugfelder, P. Pasero, and S. M. Gasser.** 2002. An N-terminal domain of Dbf4p mediates interaction with both origin recognition complex (ORC) and Rad53p and can deregulate late origin firing. Proc. Natl. Acad. Sci. USA **99:**16087–16092.
12. **Durocher, D., and S. P. Jackson.**2002. The FHA domain. FEBS Lett. **513:** 58–66.
13. **Durocher, D., I. A. Taylor, D. Sarbassova, L. F. Haire, S. L. Westcott, S. P. Jackson, S. J. Smerdon, and M. B. Yaffe.** 2000. The molecular basis of FHA domain:phosphopeptide binding specificity and implications for phospho-dependent signaling mechanisms. Mol. Cell **6:**1169–1182.
14. **Emili, A.** 1998. MEC1-dependent phosphorylation of Rad9p in response to DNA damage. Mol. Cell **2:**183–189.
15. **Emili, A., D. M. Schieltz, J. R. Yates III, and L. H. Hartwell.** 2001. Dynamic interaction of DNA damage checkpoint protein Rad53 with chromatin assembly factor Asf1. Mol. Cell **7**:13–20.
16. **Fields, S., and O. Song.** 1989. A novel genetic system to detect protein-protein interactions. Nature **340:**245–247.
17. **Hammet, A., B. L. Pike, and J. Heierhorst.** 2002. Posttranscriptional regulation of the RAD5 DNA repair gene by the Dun1 kinase and the Pan2-Pan3 poly(A)-nuclease complex contributes to survival of replication blocks. J. Biol. Chem. **277:**22469–22474.
18. **Hammet, A., B. L. Pike, C. J. McNees, L. A. Conlan, N. Tenis, and J. Heierhorst.** 2003. FHA domains as phospho-threonine binding modules in cell signaling. IUBMB Life **55:**23–27.
19. **Hammet, A., B. L. Pike, K. I. Mitchelhill, T. Teh, B. Kobe, C. M. House, B. E. Kemp, and J. Heierhorst.** 2000. FHA domain boundaries of the Dun1p and Rad53p cell cycle checkpoint kinases. FEBS Lett. **471:**141–146.
20. **Heierhorst, J., B. Kobe, S. C. Feil, M. W. Parker, G. M. Benian, K. R. Weiss, and B. E. Kemp.** 1996. Ca^{2+}/S100 regulation of giant protein kinases. Nature **380:**636–639.
21. **Huang, M., Z. Zhou, and S. J. Elledge.** 1998. The DNA replication and damage checkpoint pathways induce transcription by inhibition of the Crt1 repressor. Cell **94:**595–605.
22. **James, P., J. Halladay, and E. A. Craig.** 1996. Genomic libraries and a host strain designed for highly efficient two-hybrid selection in yeast. Genetics **144:**1425–1436.
23. **Jorgensen, P., J. L. Nishikawa, B.-J. Breitkreutz, and M. Tyers.** 2002. Systematic identification of pathways that couple cell growth and division in yeast. Science **297:**395–400.
24. **Kondo, T., K. Matsumoto, and K. Sugimoto.** 1999. Role of a complex containing Rad17, Mec3, and Ddc1 in the yeast DNA damage checkpoint pathway. Mol. Cell. Biol. **19:**1136–1143.
25. **Kumar, R., D. M. Reynolds, A. Shevchenko, S. D. Goldstone, and S. Dalton.** 2000. Forkhead transcription factors, Fkh1p and Fkh2p, collaborate with Mcm1p to control transcription required for M-phase. Curr. Biol. **10:**896–906.
26. **Lee, S. J., M. F. Schwartz, J. K. Duong, and D. F. Stern.** 2003. Rad53 phosphorylation site clusters are important for Rad53 regulation and signaling. Mol. Cell. Biol. **23:**6300–6314.
27. **Leroy, C., S. E. Lee, M. B. Vaze, F. Ochsenbien, R. Guerois, J. E. Haber, and M. C. Marsolier-Kergoat.** 2003. PP2C phosphatases Ptc2 and Ptc3 are required for DNA checkpoint inactivation after a double-strand break. Mol. Cell **11:**827–835.

28. **Li, J., G. Lee, S. R. Van Doren, and J. C. Walker.** 2000. The FHA domain mediates phosphoprotein interactions. J. Cell Sci. **113:**4143–4149.
29. **Lin, J. J., and V. A. Zakian.** 1994. Isolation and characterization of two Saccharomyces cerevisiae genes that encode proteins that bind to (TG1–3)n single strand telomeric DNA in vitro. Nucleic Acids Res. **22:**4906–4913.
30. **Mallory, J. C., and T. D. Petes.** 2000. Protein kinase activity of Tel1p and Mec1p, two Saccharomyces cerevisiae proteins related to the human ATM protein kinase. Proc. Natl. Acad. Sci. USA **97:**13749–13754.
31. **Martin, S. G., T. Laroche, N. Suka, M. Grunstein, and S. M. Gasser.** 1999. Relocalization of telomeric Ku and SIR proteins in response to DNA strand breaks in yeast. Cell **97:**621–633.
32. **Matsuoka, S., M. Huang, and S. J. Elledge.** 1998. Linkage of ATM to cell cycle regulation by the Chk2 protein kinase. Science **282:**1893–1897.
33. **Nash, P., X. Tang, S. Orlicky, Q. Chen, F. B. Gertler, M. D. Mendenhall, F. Sicheri, T. Pawson, and M. Tyers.** 2001. Multisite phosphorylation of a CDK inhibitor sets a threshold for the onset of DNA replication. Nature **414:**514–521.
34. **Navas, T. A., Z. Zhou, and S. J. Elledge.** 1995. DNA polymerase epsilon links the DNA replication machinery to the S phase checkpoint. Cell **80:**29–39.
35. **Pellicioli, A., C. Lucca, G. Liberi, F. Marini, M. Lopes, P. Plevani, A. Romano, P. P. Di Fiore, and M. Foiani.** 1999. Activation of Rad53 kinase in response to DNA damage and its effect in modulating phosphorylation of the lagging strand DNA polymerase. EMBO J. **18:**6561–6572.
36. **Pike, B. L., A. Hammet, and J. Heierhorst.** 2001. Role of the N-terminal forkhead-associated domain in the cell cycle checkpoint function of the Rad53 kinase. J. Biol. Chem. **276:**14019–14026.
37. **Pike, B. L., S. Yongkiettrakul, M. D. Tsai, and J. Heierhorst.** 2003. Diverse but overlapping functions of the two forkhead-associated (FHA) domains in Rad53 checkpoint kinase activation. J. Biol. Chem. **278:**30421–30424.
38. **Rouse, J., and S. P. Jackson.** 2002. Lcd1p recruits Mec1p to DNA lesions in vitro and in vivo. Mol. Cell **9:**857–869.
39. **Sanchez, Y., J. Bachant, H. Wang, F. Hu, D. Liu, M. Tetzlaff, and S. J. Elledge.** 1999. Control of the DNA damage checkpoint by chk1 and rad53 protein kinases through distinct mechanisms. Science **286:**1166–1171.
40. **Sanchez, Y., B. A. Desany, W. J. Jones, Q. Liu, B. Wang, and S. J. Elledge.** 1996. Regulation of RAD53 by the ATM-like kinases MEC1 and TEL1 in yeast cell cycle checkpoint pathways. Science **271:**357–360.
41. **Santocanale, C., and J. F. Diffley.** 1998. A Mec1- and Rad53-dependent checkpoint controls late-firing origins of DNA replication. Nature **395:**615–618.
42. **Schwartz, M. F., J. K. Duong, Z. Sun, J. S. Morrow, D. Pradhan, and D. F. Stern.** 2002. Rad9 phosphorylation sites couple Rad53 to the Saccharomyces cerevisiae DNA damage checkpoint. Mol. Cell **9:**1055–1065.
43. **Schwartz, M. F., S. J. Lee, J. K. Duong, S. Eminaga, and D. F. Stern.** 2003. FHA domain-mediated DNA checkpoint regulation of Rad53. Cell Cycle **2:**384–396.
44. **Sheu, Y. J., Y. Barral, and M. Snyder.** 2000. Polarized growth controls cell shape and bipolar bud site selection in *Saccharomyces cerevisiae*. Mol. Cell. Biol. **20:**5235–5247.
45. **Sidorova, J. M., and L. L. Breeden.** 1997. Rad53-dependent phosphorylation of Swi6 and down-regulation of CLN1 and CLN2 transcription occur in response to DNA damage in Saccharomyces cerevisiae. Genes Dev. **11:**3032–3045.
46. **Sun, Z., J. Hsiao, D. S. Fay, and D. F. Stern.** 1998. Rad53 FHA domain associated with phosphorylated Rad9 in the DNA damage checkpoint. Science **281:**272–274.
47. **Surana, U., H. Robitsch, C. Price, T. Schuster, I. Fitch, A. B. Futscher, and K. Nasmyth.** 1991. The role of CDC28 and cyclins during mitosis in the budding yeast S. cerevisiae. Cell **65:**145–161.
48. **Tong, A. H., M. Evangelista, A. B. Parsons, H. Xu, G. D. Bader, N. Page, M. Robinson, S. Raghibizadeh, C. W. Hogue, H. Bussey, B. Andrews, M. Tyers, and C. Boone.** 2001. Systematic genetic analysis with ordered arrays of yeast deletion mutants. Science **294:**2364–2368.
49. **Vialard, J. E., C. S. Gilbert, C. M. Green, and N. F. Lowndes.** 1998. The budding yeast Rad9 checkpoint protein is subjected to Mec1/Tel1-dependent hyperphosphorylation and interacts with Rad53 after DNA damage. EMBO J. **17:**5679–5688.
50. **Weinert, T. A., G. L. Kiser, and L. H. Hartwell.** 1994. Mitotic checkpoint genes in budding yeast and the dependence of mitosis on DNA replication and repair. Genes Dev. **8:**652–665.
51. **Zhao, X., A. Chabes, V. Domkin, L. Thelander, and R. Rothstein.** 2001. The ribonucleotide reductase inhibitor Sml1 is a new target of the Mec1/Rad53 kinase cascade during growth and in response to DNA damage. EMBO J. **20:**3544–3553.
52. **Zhao, X., E. G. Muller, and R. Rothstein.** 1998. A suppressor of two essential checkpoint genes identifies a novel protein that negatively affects dNTP pools. Mol. Cell **2:**329–340.
53. **Zhou, B. B., and S. J. Elledge.** 2000. The DNA damage response: putting checkpoints in perspective. Nature **4**8:433–439.